Drug Design, Development and Therapy

Dovepress
Taylor & Francis Group

Open Access Full Text Article

ORIGINAL RESEARCH

CXCR2 Activated JAK3/STAT3 Signaling Pathway Exacerbating Hepatotoxicity Associated with Tacrolimus

Xiao Chen[1,*], Ke Hu[2,*], Yue Zhang[2], Su-Mei He[3], Dong-Dong Wang[2]

[1]School of Nursing, Xuzhou Medical University, Xuzhou, Jiangsu, 221004, People's Republic of China; [2]Jiangsu Key Laboratory of New Drug Research and Clinical Pharmacy & School of Pharmacy, Xuzhou Medical University, Xuzhou, Jiangsu, 221004, People's Republic of China; [3]Department of Pharmacy, Suzhou Research Center of Medical School, Suzhou Hospital, Affiliated Hospital of Medical School, Nanjing University, Suzhou, Jiangsu, 215153, People's Republic of China

*These authors contributed equally to this work

Correspondence: Su-Mei He, Department of Pharmacy, Suzhou Research Center of Medical School, Suzhou Hospital, Affiliated Hospital of Medical School, Nanjing University, Suzhou, Jiangsu, 215153, People's Republic of China, Email hehe8204@163.com; Dong-Dong Wang, Jiangsu Key Laboratory of New Drug Research and Clinical Pharmacy & School of Pharmacy, Xuzhou Medical University, Xuzhou, Jiangsu, 221004, People's Republic of China, Email 13852029591@163.com

Purpose: Tacrolimus could induce hepatotoxicity during clinical use, and the mechanism was still unclear, which posed new challenge for the prevention and treatment of tacrolimus-induced hepatotoxicity. The aim of this study was to investigate the mechanism of tacrolimus-induced hepatotoxicity and provide reference for drug development target.

Methods: In this study, biochemical analysis, pathological staining, immunofluorescent staining, immunohistochemical staining, transcriptomic analysis, Western blotting was used to investigate the mechanism of tacrolimus-induced hepatotoxicity in gene knockout mice and Wistar rats.

Results: In gene knockout mice, compared to wild-type mice, CXCR2-deficiency alleviated tacrolimus-induced hepatotoxicity ($P < 0.05$ or $P < 0.01$). In Wistar rats, compared to control group, CXCL2-CXCR2, JAK3/STAT3 signaling pathway (phosphorylation of JAK3 and STAT3) were up-regulated, the expression of CIS was lowered and the expression of PIM1 was raised, inducing liver pathological change ($P < 0.05$ or $P < 0.01$); Inversely, blocking CXCR2 could reverse the expression of p-JAK3/p-STAT3 and tacrolimus-induced hepatotoxicity ($P < 0.05$ or $P < 0.01$).

Conclusion: CXCR2 activated JAK3/STAT3 signaling pathway (phosphorylation of JAK3 and STAT3) exacerbating hepatotoxicity associated with tacrolimus, meanwhile the expression of CIS was down-regulated, the expression of PIM1 was up-regulated. Blocking CXCR2 could reverse the expression of p-JAK3/p-STAT3, CIS, PIM1, and tacrolimus-induced hepatotoxicity.

Keywords: CXCR2, JAK3/STAT3 signaling pathway, hepatotoxicity, tacrolimus, CIS, PIM1

Introduction

Tacrolimus was approved in the United States in April 1994 for the prevention of organ rejection after liver transplantation.[1] In addition, it could be used for kidney transplantation,[2] heart transplantation,[3] lung transplantation,[4] hematopoietic stem cell transplantation,[5] juvenile idiopathic arthritis,[6] refractory nephrotic syndrome,[7] myasthenia gravis,[8] ulcerative colitis,[9] systemic lupus erythematosus,[10] lupus nephritis[11] and autoimmune hepatitis.[12] However, due to the narrow therapeutic window of tacrolimus and large inter-individual and intra-individual pharmacokinetic variation, there were differences in the range of therapeutic windows required in the treatment of different diseases, where too low drug concentration would increase rejection or poor treatment of disease, while too high drug concentration may lead to adverse reactions and even toxicity,[1,13] such as nephrotoxicity, neurotoxicity, infection, tumor, diabetes and gastrointestinal reactions.[14,15] Therefore, it was challenging to achieve individual and precise administration of tacrolimus in clinical practice[16,17] and it was urgent to achieve precise clinical treatment of tacrolimus.

Received: 13 September 2024
Accepted: 19 December 2024
Published: 28 December 2024

Graphical Abstract

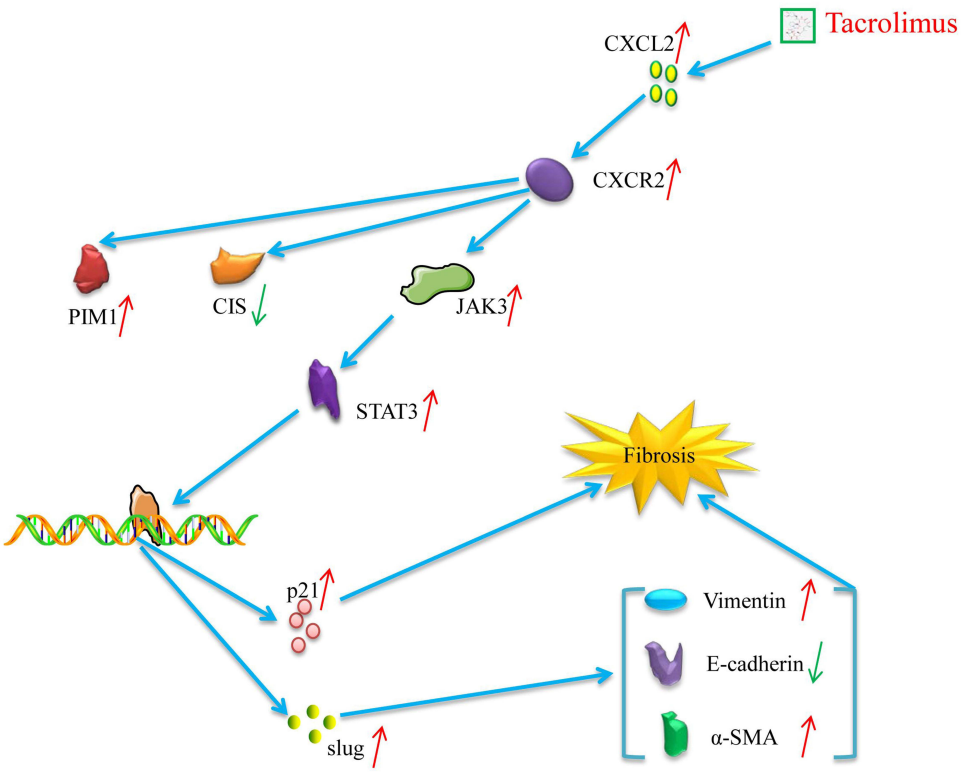

In the early stage, based on therapeutic drug monitoring (TDM), pharmacogenomics (PGx) and model-informed precision medicine,[18] we systematically constructed quantitative pharmacological models of tacrolimus in lung transplantation,[19] liver transplantation,[20] kidney transplantation[21] and hematopoietic stem cell transplantation,[22–24] and the precise administration of tacrolimus in patients was basically achieved. However, tacrolimus could induce hepatotoxicity during clinical use,[25–30] and the mechanism was still unclear, which also posed new challenge for the prevention and treatment of tacrolimus-induced hepatotoxicity.

Our preliminary research confirmed that tacrolimus increased the expression level of chemokine receptor CXCR2 to promote nephrotoxicity,[15] however, whether CXCR2 was activated in tacrolimus-induced hepatotoxicity, and whether it played an important role, was unclear. Thus, the present study would furtherly explore the potential target of tacrolimus-induced hepatotoxicity based on CXCR2, and provided idea for drug prevention and treatment of tacrolimus-induced hepatotoxicity.

Materials and Methods

Animal Models

In the animal experiment part, this study carried out the research of knockout mice and Wistar rats, respectively. CXCR2-deficient (CXCR2-KO) mice and wild-type (WT) mice were purchased from Cyagen Biosciences, and Wistar rats were purchased from Vital River Laboratory Animal Technology Co., Ltd. Tacrolimus (5A3486C) was purchased from Astellas Ireland Co., Ltd and CXCR2 antagonist (SB225002) was purchased from Selleck.

Twelve CXCR2-KO mice were randomly divided into control (N-KO) group (n=6) and tacrolimus intervention (T-KO) group (n=6). Meanwhile, the control WT mice were also divided into control (N-WT) group (n=6) and tacrolimus intervention (T-WT) group (n=6). N-KO group, T-KO group, N-WT group and T-WT group were all half

male and half female. 3 mg/kg/day tacrolimus was used to intervene T-KO and T-WT groups via intraperitoneal injection for two weeks, and equal volume of normal saline was used to intervene N-KO and N-WT groups in the same way.

Twenty-four male Wistar rats were randomly divided into control (N) group (n=8), tacrolimus intervention (T) group (n=8), and CXCR2 antagonist (C) group (n=8). 2 mg/kg/day tacrolimus was used to intervene T and C groups via intraperitoneal injection and equal volume of normal saline was used to intervene N group, meanwhile, 2 mg/kg/day CXCR2 antagonist was used to intervene C group via intraperitoneal injection and equal volume of normal saline was used to intervene N and T groups. This part of the intervention lasted two weeks.

The above research was approved by *The Animal Care and Use Committee of Xuzhou Medical University* (No.202208S030). In addition, we complied with *Guideline for Ethical Review of Animal Welfare* (GB/T 35892–2018) to ensure the welfare of the experimental animals used in our research.

Sample Collection

When the intervention was over for 2 weeks, mice and rats were all sacrificed and blood sample and liver were collected. The fresh liver was fixed using paraformaldehyde, and the residual liver tissues along with blood sample were rapidly freezed using liquid nitrogen.

Biochemical Index Detection

The biochemical index was tested, including alanine transaminase (ALT), aspartate transaminase (AST), total bilirubin (TBIL), superoxide dismutase (SOD), malondialdehyde (MDA), and glutathione peroxidase (GSH-Px). ALT kit (S03030), and AST (S03040) were purchase from Rayto Life and Analytical Sciences Co., Ltd. TBIL kit (C120) was purchase from Changchun Huili Biotech Co., Ltd. SOD kit (A001-1), MDA kit (A003-1), and GSH-Px kit (A005) were purchase from Nanjing Jiancheng Bioengineering Institute. Refer to the instructions of the above kits for operation.

Pathological Staining

Masson staining, sirius red staining were used to analyze the pathological change of liver. Masson dye kit (G1006), and sirius red dye (G1018) were purchase from Servicebio Biotechnology (Wuhan) Co., Ltd. Take pictures with the pathological section scanner (3DHISTECH Pannoramic, version: Pannoramic MIDI) and mean of integral optical density (IOD) was used to quantify the results and calculate with Image-Pro Plus 6.0 software (Media Cybernetics, Inc).

Immunofluorescent Staining

Phosphorylation of JAK3 and STAT3 were the main active protein forms of JAK3/STAT3 signaling pathway, and in this study, we explored the expression of p-JAK3 and p-STAT3. Immunofluorescent staining was used to measure the expression of E-cadherin, α-SMA, CXCL2, CXCR2, p-JAK3, p-STAT3, p21, slug, PIM1. Antibodies against E-cadherin (GB12082), α-SMA (GB13044) were purchased from Servicebio Biotechnology (Wuhan) Co., Ltd. CXCL2 (PY88673), CXCR2 (TD7095), p-JAK3 (TA8160), p-STAT3 (T56566), p21 (T55543), slug (MG774907), PIM1 (TA0844) were purchased from Abmart Medical Technology (Shanghai) Co., Ltd. Take pictures with the pathological section scanner and mean of IOD was used to quantify the results and calculate with Image-Pro Plus 6.0 software.

Immunohistochemical Staining

Immunohistochemical staining was used to measure the expression of vimentin, COL-1, COL-3, FN, CIS. Antibodies against vimentin (GB11192), COL-1 (GB11022), COL-3 (GB111629), FN (GB114491) were purchased from Servicebio Biotechnology (Wuhan) Co., Ltd. Antibody against CIS (PU781105) was purchased from Abmart Medical Technology (Shanghai) Co., Ltd. Take pictures with the pathological section scanner and mean of IOD was used to quantify the results and calculate with Image-Pro Plus 6.0 software.

Transcriptomic Analysis

Transcriptome sequencing included RNA extraction, quality detection, library construction, library quality control, sequencing, gene expression quantitative analysis, gene differential expression analysis, functional enrichment analysis,

etc. Sequencing data were analyzed as raw reads, and were saved in a FASTQ format document. In this project, the HISAT2 software was used to sequence Clean Reads with a specified genome to obtain information about their location on the reference genome. This project used genomic version: Rattus_norvegicus_Ensembl_104. The FPKM value of each gene's expression in each sample was calculated using featureCounts software. DESeq2 was used to analyze the differential expression of genes. With KEGG pathway as the unit and reference genome as the background, Fisher's Exact Test was used to analyze and calculate the significance level of gene enrichment in each pathway, so as to identify the metabolic and signal transduction pathways that were significantly affected. GSEA ranked all genes according to the degree of differential expression between the two groups of samples, and then used statistical methods to check whether the predefined set of genes was enriched at the top or bottom of the ranking table In this study, the results of protein interaction network analysis and pathway annotation were combined to obtain a more comprehensive and systematic molecular level cell activity model, which was convenient for further research and exploration of molecular mechanisms. We mainly applied the interaction relationship in the STRING protein interaction database, and directly extracted the interaction relationship of the target gene set from the database to build a network.

Western Blotting

Western blotting was used to measure the expression of CXCL2, CXCR2, vimentin, E-cadherin, α-SMA, p-JAK3, p-STAT3, p21, PIM1, CIS, slug. Antibodies against CXCL2 (PY88673), vimentin (T55134), E-cadherin (TA0131), α-SMA (T55295), p-STAT3 (T56566), p21 (PA9426), PIM1 (TA0844), CIS (PU781105), slug (MG774907) were purchased from Abmart Medical Technology (Shanghai) Co., Ltd.

Antibody against CXCR2 (ab65968) was purchased from Abcam. Antibody against p-JAK3 (AF8160) was purchased from Affinity Biosciences. Antibodies against GAPDH (60004-1-Ig) and β-actin (66009-1-Ig) were purchased from Proteintech. Western blotting was tested with chemiluminescence gel imager (Tanon, Tanon-4600) and results were used for semi-quantitative analysis.

Statistical Analysis

T-test was used for the comparison of two groups and one-way ANOVA was used for the comparison of three groups using SPSS software (IBM, Version 23), where *P*-value <0.05 or *P*-value <0.01 were considered to indicate a statistically significant difference.

Results

CXCR2-Deficiency Alleviated Tacrolimus-Induced Hepatotoxicity

Figure 1A was flow diagram, Figure 1B–G were ALT, AST, TBIL, SOD, MDA, and GSH-Px, respectively. There were no significant differences in N-WT group and N-KO group from the levels of ALT, AST, TBIL, SOD, MDA, and GSH-Px. The levels of ALT, AST, TBIL, MDA were significantly increased ($P < 0.05$ or $P < 0.01$) in T-WT group compared to N-WT group, and compared to T-WT group the levels of ALT, AST, TBIL, MDA were significantly decreased ($P < 0.05$ or $P < 0.01$) in T-KO group. The levels of SOD and GSH-Px were significantly decreased ($P < 0.05$ or $P < 0.01$) in T-WT group compared to N-WT group, and compared to T-WT group the levels of SOD and GSH-Px were significantly increased ($P < 0.01$) in T-KO group. Masson staining, E-cadherin/α-SMA fluorescent staining, and corresponding quantitative analysis results were shown in Figure 1H–K, where the degree of liver fibrosis, and expression quantities of E-cadherin and α-SMA were no significant difference in N-WT group and N-KO group. The degree of liver fibrosis, and expression quantity of α-SMA were significantly increased ($P < 0.01$) in T-WT group compared to N-WT group, and compared to T-WT group the degree of liver fibrosis, and expression quantity of α-SMA were significantly decreased ($P < 0.01$) in T-KO group. For another, the expression quantity of E-cadherin was significantly decreased ($P < 0.01$) in T-WT group compared to N-WT group and compared to T-WT group the expression quantity of E-cadherin was significantly increased ($P < 0.01$) in T-KO group.

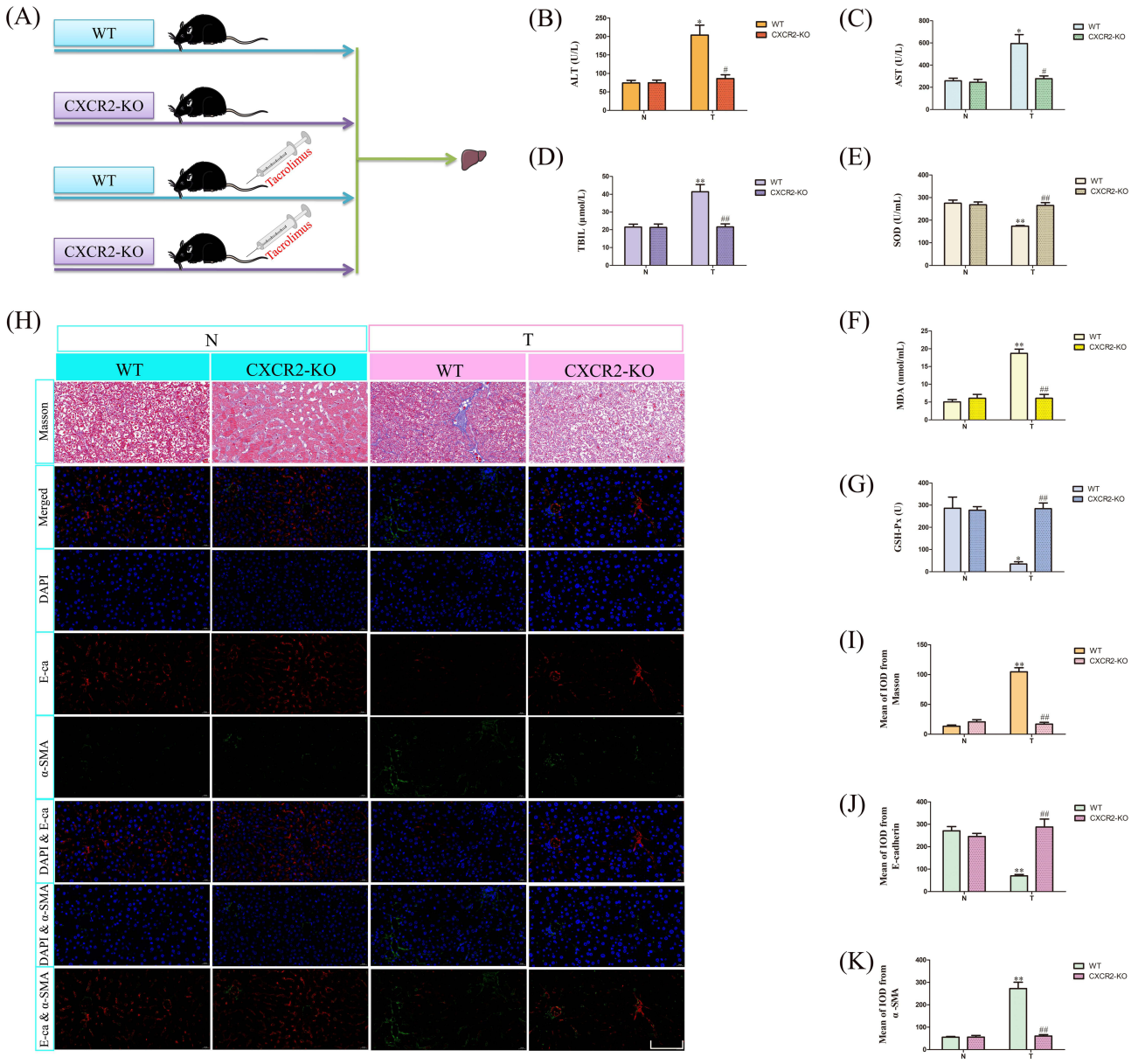

Figure 1 CXCR2-deficiency alleviated tacrolimus-induced hepatotoxicity. (**A**) Flow diagram. (**B**) ALT. (**C**) AST. (**D**) TBIL. (**E**) SOD. (**F**) MDA. (**G**) GSH-Px. (**H**) Masson staining and E-cadherin/α-SMA fluorescent staining. (**I**) Mean of IOD from Masson. (**J**) Mean of IOD from E-cadherin. (**K**) Mean of from α-SMA. $^{*}P < 0.05$, $^{**}P < 0.01$ vs N-WT, $^{\#}P < 0.05$, $^{\#\#}P < 0.01$ vs T-WT. WT, wild-type mice. CXCR2-KO, CXCR2 knockout mice. N, control group. T, tacrolimus intervention group. IOD, integral optical density. Scale bar, 100 μm.

CXCL2-CXCR2 Was Up-Regulated in Tacrolimus-Induced Hepatotoxicity

Figure 2A was flow diagram, Figure 2B–E was fluorescent staining and Western blotting of CXCL2/CXCR2. CXCL2-CXCR2 was up-regulated ($P < 0.05$ or $P < 0.01$) in T group compared to N group.

Pathological Change of Tacrolimus-Induced Hepatotoxicity

Figure 3A was Masson staining, sirius red staining and immunohistochemical staining from vimentin, COL-1, COL-3, FN, revealing increased liver fibrosis in T group compared to N group. Figure 3B was E-cadherin/α-SMA fluorescent staining, revealing the decrease of E-cadherin and increase of α-SMA in T group compared to N group. Figure 3C–F were Western blotting of vimentin, E-cadherin and α-SMA and corresponding quantitative analysis, where the expression

https://doi.org/10.2147/DDDT.S496195

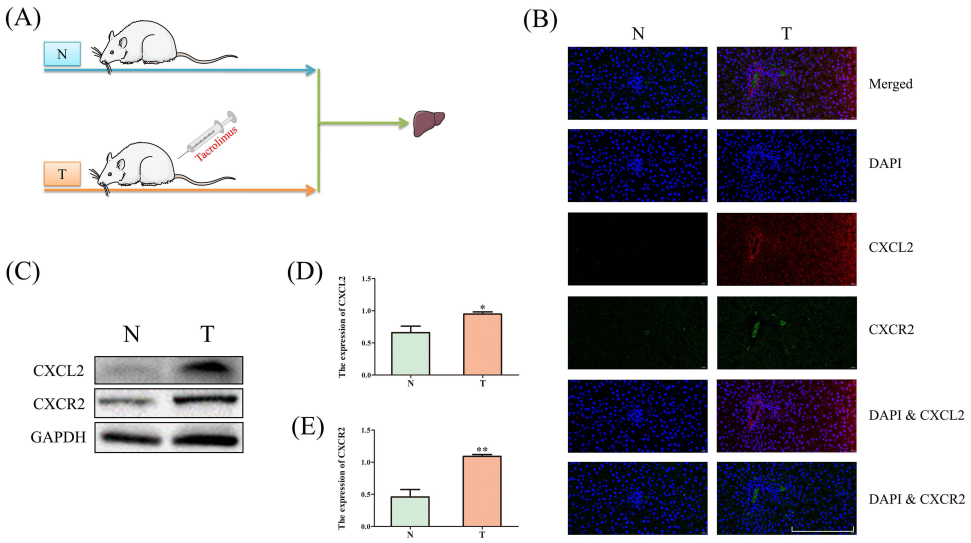

Figure 2 CXCL2-CXCR2 was up-regulated in tacrolimus-induced hepatotoxicity. (**A**) Flow diagram. (**B**) Fluorescent staining of CXCL2/CXCR2. (**C**) Western blotting of CXCL2 and CXCR2. (**D**) The expression of CXCL2. (**E**) The expression of CXCR2. **P* < 0.05, ***P* < 0.01 vs N. N, control group. T, tacrolimus intervention group. Scale bar, 200 μm.

of vimentin and α-SMA were significantly increased ($P < 0.05$ or $P < 0.01$) in T group compared to N group, and the expression of E-cadherin was significantly decreased ($P < 0.01$) in T group compared to N group.

Transcriptomic Analysis of Tacrolimus-Induced Hepatotoxicity

Figure 4A–J were density map, violin plot, Pearson correlation between samples, differential gene cluster map, volcano map of differential gene expression distribution, statistical histogram of differentially expressed genes, GSEA enrichment analysis, KEGG pathways enrichment, JAK-STAT signaling pathway, and interaction network map of differentially expressed genes, respectively. A total of 603 genes were changed in expression, 333 genes were up-regulated and 270 genes were down-regulated. Further, the present study indicated JAK3/STAT3 signaling pathway may be activated in tacrolimus-induced hepatotoxicity.

JAK3/STAT3 Signaling Pathway Was Activated in Tacrolimus-Induced Hepatotoxicity

Figure 5A–D were Western blotting of p-JAK3, p-STAT3, p21 and corresponding quantitative analysis results, where the expression of p-JAK3, p-STAT3, p21 were significantly increased ($P < 0.05$ or $P < 0.01$) in T group compared to N group. Figure 5E–H were Western blotting of PIM1, CIS, and slug and corresponding quantitative analysis results, where the expression of PIM1, slug were significantly increased ($P < 0.01$) in T group compared to N group, and the expression of CIS was significantly decreased ($P < 0.01$) in T group compared to N group. Figure 5I was the hypothesis of CXCR2 activating JAK3/STAT3 signaling pathway in tacrolimus-induced hepatotoxicity.

CXCR2 Antagonist Alleviated Tacrolimus-Induced Hepatotoxicity

Figure 6A was flow diagram, Figure 6B–G were ALT, AST, TBIL, SOD, MDA, and GSH-Px, respectively. The levels of ALT, AST, TBIL, MDA were significantly increased ($P < 0.01$) in T group compared to N group, and compared to T group the levels of ALT, AST, TBIL, MDA were significantly decreased ($P < 0.01$) in C group. The levels of SOD and GSH-Px were significantly decreased ($P < 0.01$) in T group compared to N group, and compared to T group the levels of SOD and GSH-Px were significantly increased ($P < 0.01$) in C group. Figure 6H–K were Western blotting of E-cadherin, α-SMA, vimentin and corresponding quantitative analysis results, where the expression of E-cadherin was significantly decreased ($P < 0.05$) in T group compared to N group, and compared to T group the expression of E-cadherin was significantly increased ($P < 0.01$) in C group. On the other hand, the expression of α-SMA, vimentin were significantly increased ($P < 0.01$) in T group compared to N group, and compared to T group the expression of α-SMA, vimentin were significantly decreased ($P < 0.05$ or $P < 0.01$) in C group.

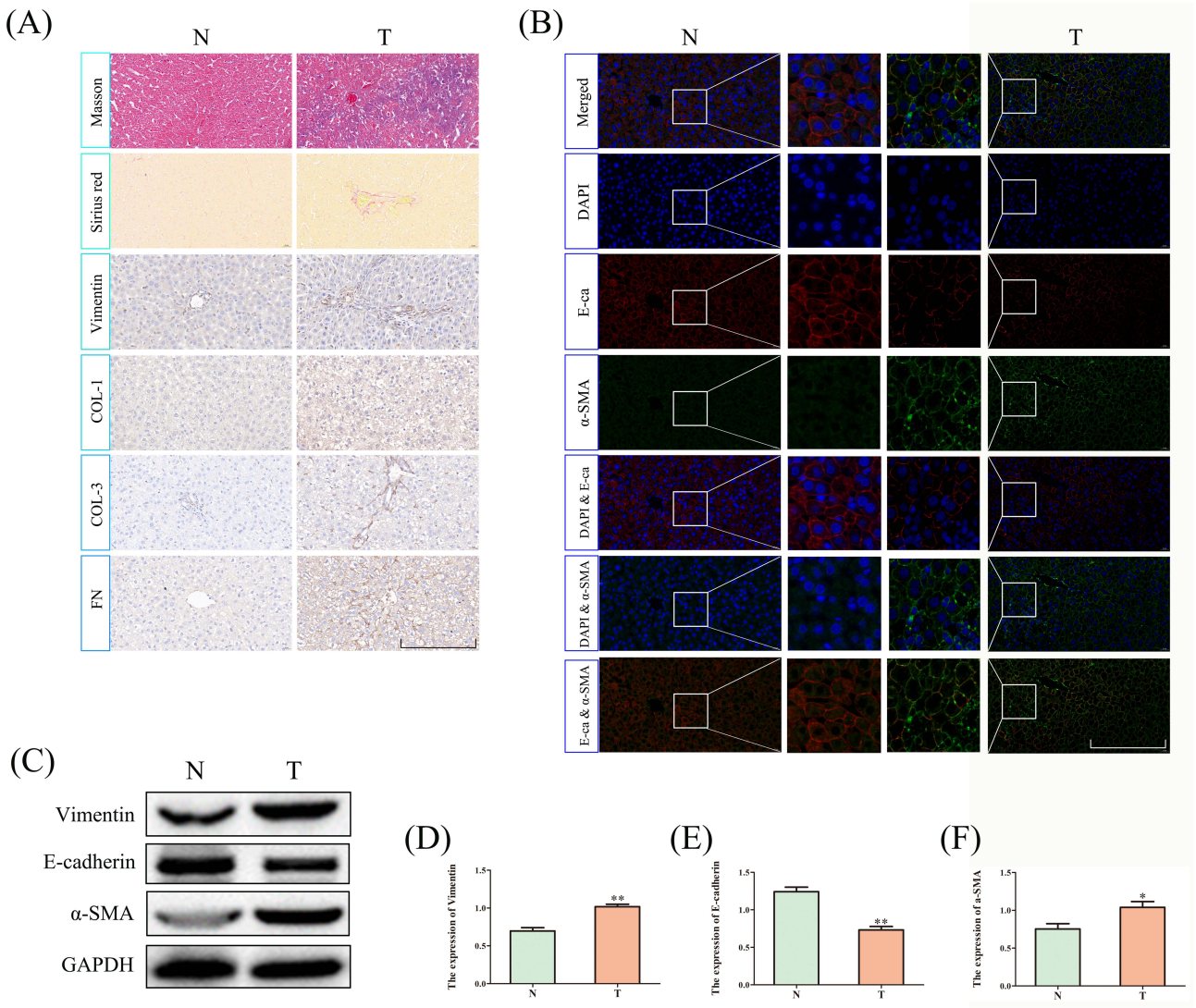

Figure 3 Pathological change of tacrolimus-induced hepatotoxicity. (**A**) Masson staining, sirius red staining and immunohistochemical staining from vimentin, COL-1, COL-3, FN. (**B**) E-cadherin/α-SMA fluorescent staining. (**C**) Western blotting of vimentin, E-cadherin and α-SMA. (**D**) The expression of vimentin. (**E**) The expression of E-cadherin. (**F**) The expression of α-SMA. *$P < 0.05$, **$P < 0.01$ vs N. N, control group. T, tacrolimus intervention group. Scale bar, 200 μm.

CXCR2 Antagonist Down-Regulating JAK3/STAT3 Signaling Pathway in Tacrolimus-Induced Hepatotoxicity

Figure 7A–H were Western blotting of p-JAK3, p-STAT3, p21, PIM1, CIS, slug and corresponding quantitative analysis results, where the expression of p-JAK3, p-STAT3, p21, PIM1, slug were significantly increased ($P < 0.05$ or $P < 0.01$) in T group compared to N group, and compared to T group the expression of p-JAK3, p-STAT3, p21, PIM1, slug were significantly decreased ($P < 0.05$ or $P < 0.01$) in C group. On the other hand, the expression of CIS was significantly decreased ($P < 0.05$) in T group compared to N group, and compared to T group the expression of CIS was significantly increased ($P < 0.01$) in C group. Figure 7I was the fluorescent staining of p-JAK3, p-STAT3, p21, slug, PIM1 and immunohistochemical staining of CIS, verifying the conclusion of corresponding Western blotting again.

CXCR2 Activated JAK3/STAT3 Signaling Pathway Exacerbating Hepatotoxicity Associated with Tacrolimus

Figure 8 was mechanism drawing, indicating CXCR2 activating JAK3/STAT3 signaling pathway (phosphorylation of JAK3 and STAT3) in tacrolimus-induced hepatotoxicity. In an overall view, CXCR2 activated JAK3/STAT3 signaling

https://doi.org/10.2147/DDDT.S496195

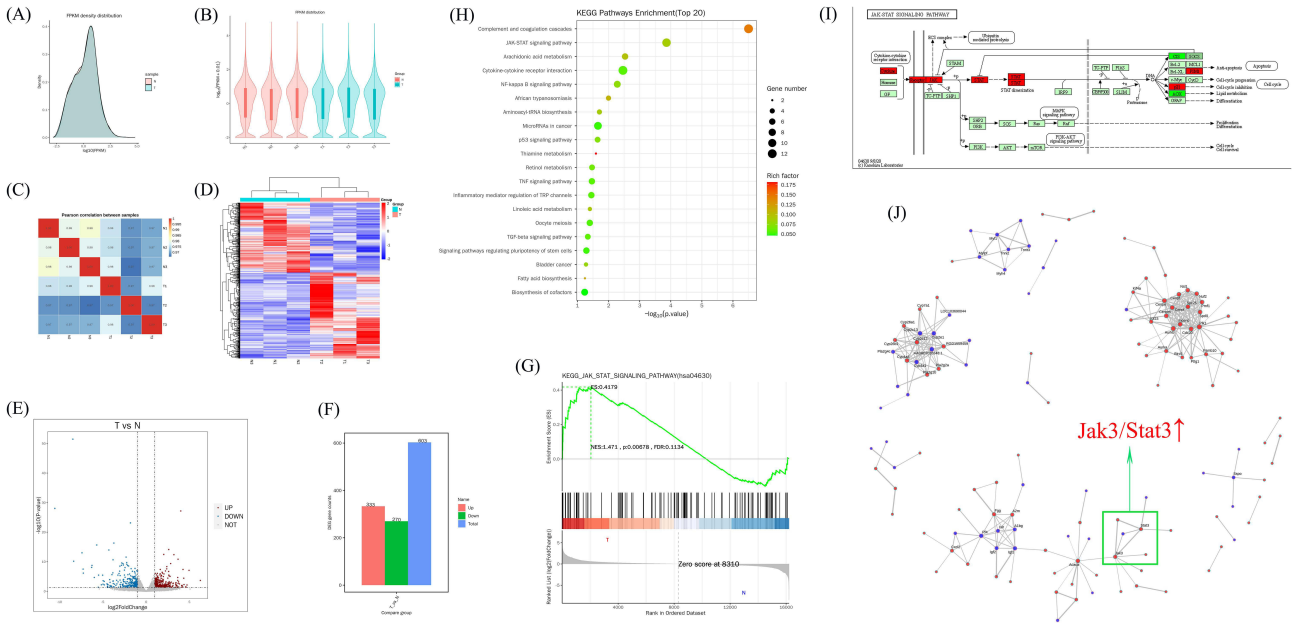

Figure 4 Transcriptomic analysis of tacrolimus-induced hepatotoxicity. (**A**) Density map. (**B**) Violin plot. (**C**) Pearson correlation between samples. (**D**) Differential gene cluster map. (**E**) Volcano map of differential gene expression distribution. (**F**) Statistical histogram of differentially expressed genes. (**G**) GSEA enrichment analysis. (**H**) KEGG pathways enrichment. (**I**) JAK-STAT signaling pathway. (**J**) Interaction network map of differentially expressed genes.

pathway (p-JAK3/p-STAT3) exacerbating hepatotoxicity associated with tacrolimus, meanwhile, the expression of CIS was down-regulated, the expression of PIM1 was up-regulated. Blocking CXCR2 could reverse the expression of p-JAK3/p-STAT3, CIS, PIM1, and tacrolimus-induced hepatotoxicity.

Discussion

Tacrolimus, a macrolide antibiotic first purified from *Streptomyces* metabolites in 1984, was an immunosuppressant. By binding with plasma FK506 binding protein, tacrolimus inhibited the activity of calcineurin in T lymphocytes, weakened the dephosphorylation of related nuclear transcription factors when lymphocytes were activated, prevented nuclear transcription factors from entering the nucleus, and then blocked the production of lymphokine by T lymphocytes, thus playing an immunosuppressive role.[31,32] In addition, tacrolimus was a substrate for the transporter P-gp, which was rapidly absorbed in most individuals after oral administration,[33] with a low bioavailability of 25% on average,[34] and binded to red blood cells and plasma proteins after entered into blood (99% of the plasma tacrolimus binded to α1 acidic glycoprotein and albumin).[35,36] Tacrolimus was metabolized by the cytochrome P450 system (CYP3A4 and CYP3A5 types) in the liver and small intestine and was excreted primarily through bile.[33] Tacrolimus had a narrow therapeutic window, blood drug concentration was closely related to efficacy and adverse reactions, and individual pharmacokinetics varied greatly and was affected by multiple factors.[37–40] At the same time, tacrolimus could induce liver toxicity during clinical use,[25–30] but the mechanism was still unclear.

In this study, we found that CXCL2-CXCR2 was up-regulated in tacrolimus-induced hepatotoxicity model. CXCR2 belonged to the CXCR family and was expressed in various cell types, including monocytes, neutrophils, mast cells, oligodendrocytes, eosinophils and endothelial cells.[41] The known ligands of CXCR2 included CXCL1, CXCL2, CXCL3, CXCL5, CXCL6, CXCL7, and CXCL8. CXCR2 belonged to a large family of GPCR, which had more than 800 receptors in humans and were associated with many human diseases. It was estimated that 30–40% of drugs targeted GPCR, and so far, the structure of several human GPCR had been identified, including the chemokine receptor CXCR1, where CXCR2 shared 78% sequence homology with CXCR1 and had a similar affinity to IL-8 binding. However, CXCR1 only binded to CXCL6 and CXCL8, indicating that CXCR2 interacted with more chemokines, had higher affinity, and played a more important role in cell chemotaxis.[41]

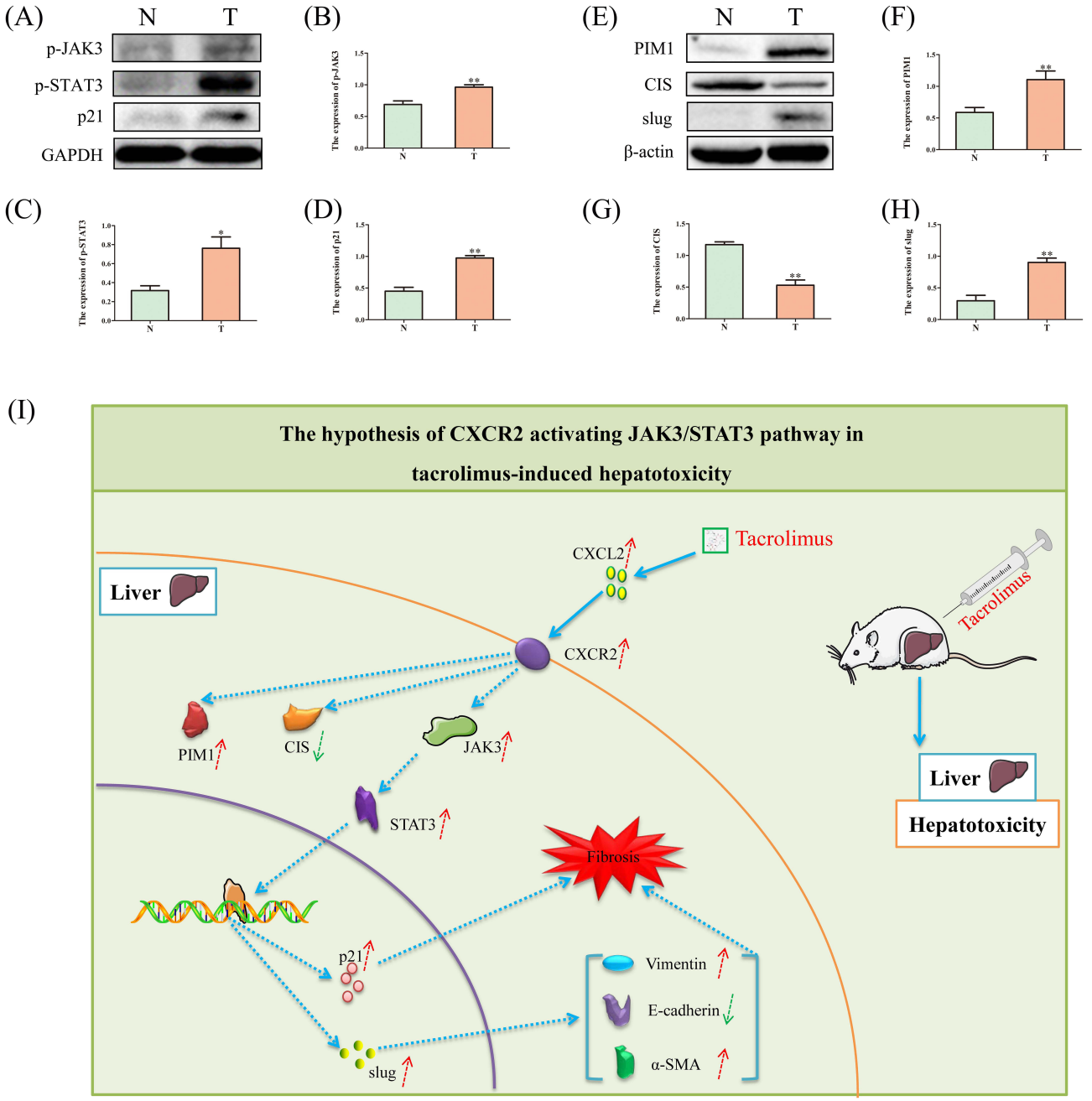

Figure 5 JAK3/STAT3 signaling pathway was activated in tacrolimus-induced hepatotoxicity. (**A**) Western blotting of p-JAK3, p-STAT3, and p21. (**B**) The expression of p-JAK3. (**C**) The expression of p-STAT3. (**D**) The expression of p21. (**E**) Western blotting of PIM1, CIS, and slug. (**F**) The expression of PIM1. (**G**) The expression of CIS. (**H**) The expression of slug. (**I**) The hypothesis of CXCR2 activating JAK3/STAT3 signaling pathway in tacrolimus-induced hepatotoxicity. The red and green arrows represented the expression of proteins after tacrolimus intervention, where the red arrows facing up meant the expression of proteins were up-regulated, the green arrows facing down meant the expression of proteins were down-regulated. JAK3 and STAT3 referred to their phosphorylated forms (p-JAK3 and p-STAT3). *$P < 0.05$, **$P < 0.01$ vs N. N, control group. T, tacrolimus intervention group.

In addition, CXCR2 and its ligands were involved in the occurrence and development of tumors and various inflammatory diseases.[42,43] In the pancreatic cancer model, high levels of CXCR2 expression were observed in both stromal and epithelial cells.[44] In addition, CXCR2 was also highly expressed in other types of tumors, such as melanoma,[45] breast cancer,[46] lung cancer,[47] kidney cancer,[48] bladder cancer,[49] prostate cancer[50] and rectal cancer.[51] In terms of drug-induced organ toxicity, it was currently known that tacrolimus increased the expression level of CXCR2 to promote renal fibrosis progression,[15] CXCR2 up-regulation played an important role in cyclophosphamide-induced

https://doi.org/10.2147/DDDT.S496195

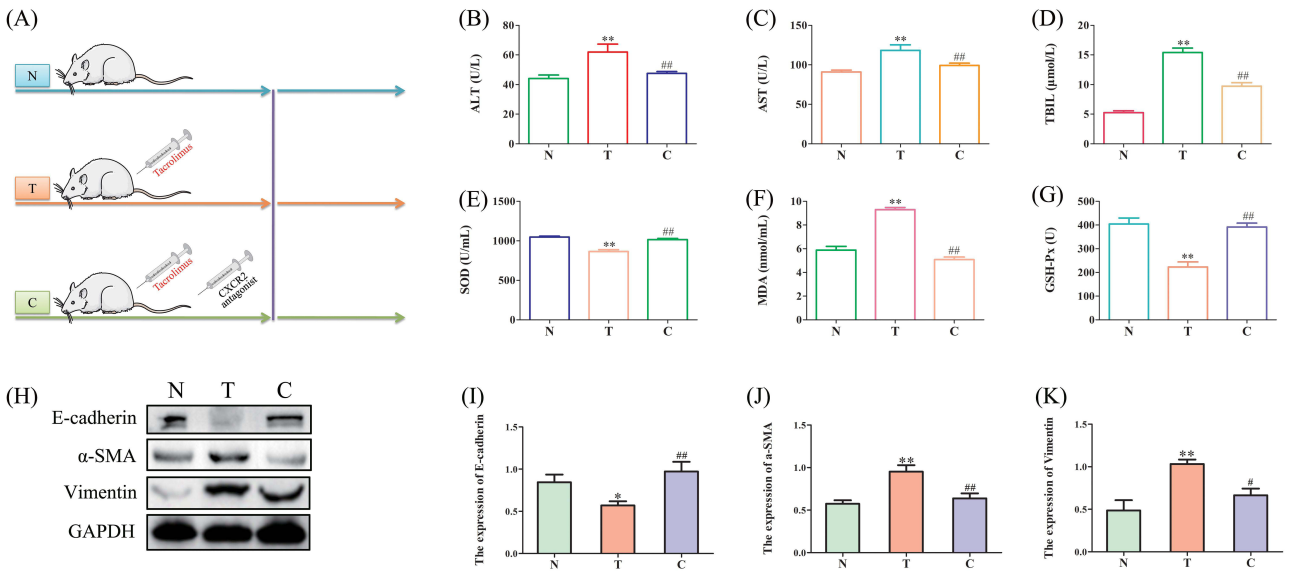

Figure 6 CXCR2 antagonist alleviated tacrolimus-induced hepatotoxicity. (**A**) Flow diagram. (**B**) ALT. (**C**) AST. (**D**) TBIL. (**E**) SOD. (**F**) MDA. (**G**) GSH-Px. (**H**) Western blotting of E-cadherin, α-SMA, and vimentin. (**I**) The expression of E-cadherin. (**J**) The expression of α-SMA. (**K**) The expression of vimentin. **P* < 0.05, ***P* < 0.01 vs N; $^{\#}P$ < 0.05, $^{\#\#}P$ < 0.01 vs T; N, control group. T, tacrolimus intervention group. C, CXCR2 antagonist group.

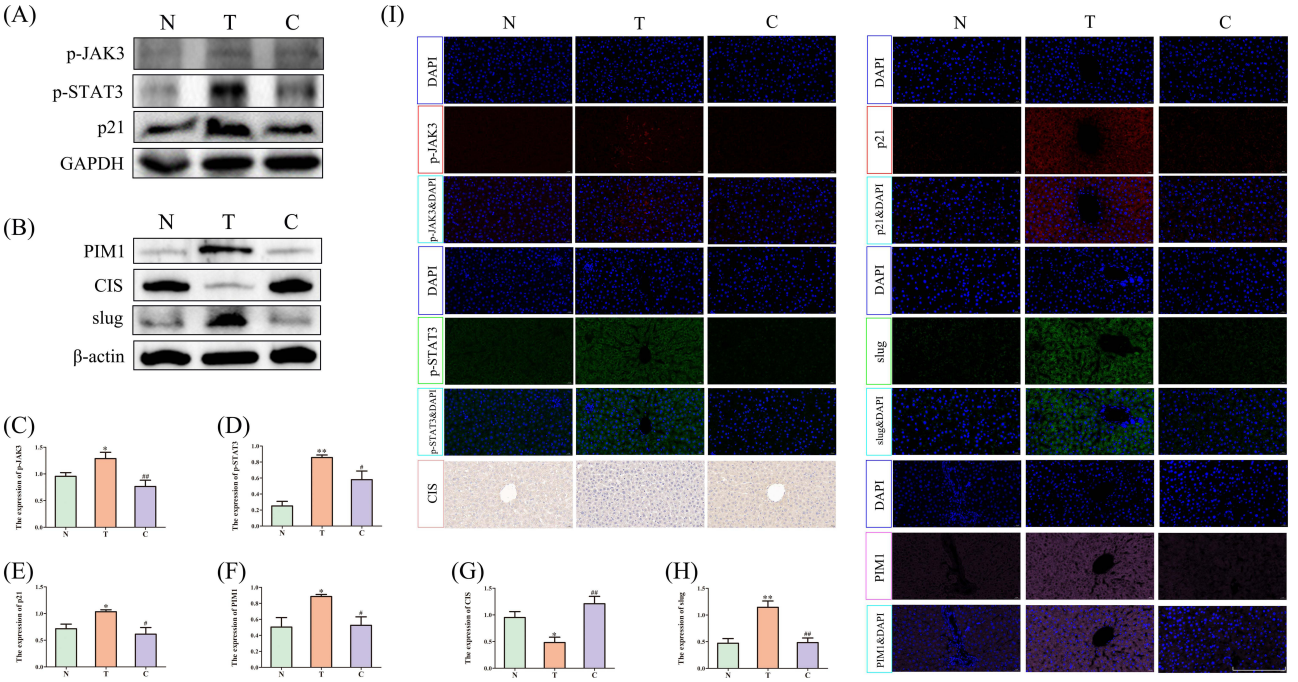

Figure 7 CXCR2 antagonist down-regulated JAK3/STAT3 signaling pathway in tacrolimus-induced hepatotoxicity. (**A**) Western blotting of p-JAK3, p-STAT3, and p21. (**B**) Western blotting of PIM1, CIS, and slug. (**C**) The expression of p-JAK3. (**D**) The expression of p-STAT3. (**E**) The expression of p21. (**F**) The expression of PIM1. (**G**) The expression of CIS. (**H**) The expression of slug. (**I**) Fluorescent staining of p-JAK3, p-STAT3, p21, slug, PIM1 and immunohistochemical staining of CIS. **P* < 0.05, ***P* < 0.01 vs N; $^{\#}P$ < 0.05, $^{\#\#}P$ < 0.01 vs T; N, control group. T, tacrolimus intervention group. C, CXCR2 antagonist group. Scale bar, 200 μm.

cystitis in rats and may be a potential target for the treatment of drug-induced cystitis.[52] In mice, knocking out CXCR2 could prevent kidney injury induced by sodium dextran sulfate.[53] Thus, it was concluded that CXCR2 up-regulation was a biological signal of danger in tumor, inflammation and clinical drug toxicity.

Studies had shown that ligand-binding CXCR2 could activate multiple G-protein regulatory cascade signals, including Ras/Erk, PI3K/Akt, PLC/PKC, MAPK/p38, JAK3/STAT3 and other signaling pathways.[41] In the present study, it was

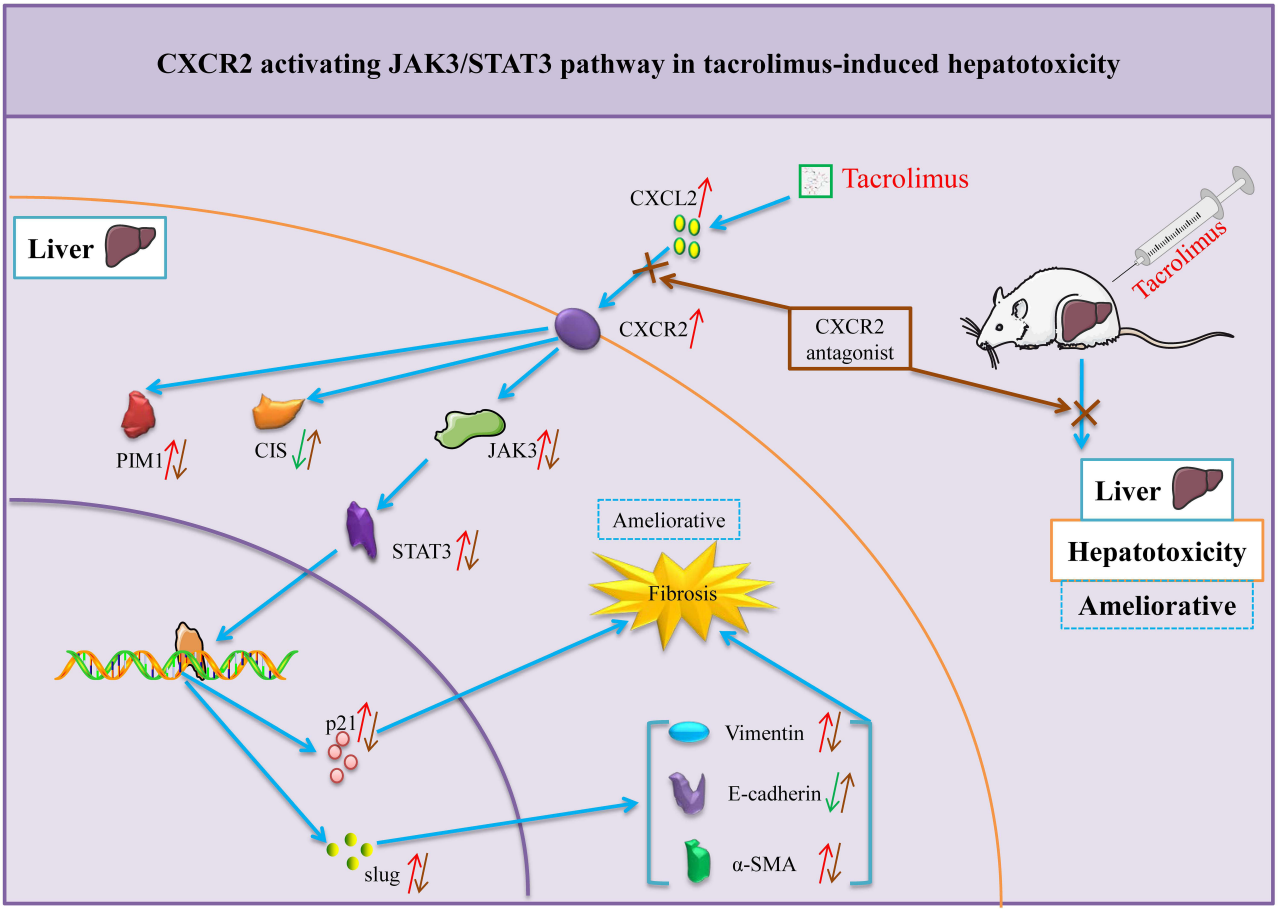

Figure 8 CXCR2 activated JAK3/STAT3 signaling pathway exacerbating hepatotoxicity associated with tacrolimus. The red and green arrows represented the expression of proteins after tacrolimus intervention, where the red arrows facing up meant the expression of proteins were up-regulated, the green arrows facing down meant the expression of proteins were down-regulated. The brown arrows represented the expression of proteins after CXCR2 antagonist intervention, where the arrows facing up meant the expression of proteins were up-regulated, the arrows facing down meant the expression of proteins were down-regulated. JAK3 and STAT3 referred to their phosphorylated forms (p-JAK3 and p-STAT3).

found that JAK3/STAT3 signaling pathway was up-regulated in tacrolimus-induced hepatotoxicity, which induced the up-regulated expression of p21 and slug, and induced liver fibrosis. At the same time, the expression of CIS was lowered and the expression of PIM1 was raised. JAK3/STAT3 signaling pathway had been found to play an important role in the occurrence, development and prevention of a variety of diseases. Xiao et al reported ameliorative effect of alangium chinense (Lour). Harms on rheumatoid arthritis by reducing autophagy with targeting regulate JAK3-STAT3 and COX-2 pathways.[54] Zhang et al reported single-cell analysis highlighted a population of Th17-polarized $CD4^+$ naïve T cells showing IL6/JAK3/STAT3 activation in pediatric severe aplastic anemia.[55] Fathi et al reported mesenchymal stem cells caused induction of granulocyte differentiation of rat bone marrow C-kit^+ hematopoietic stem cells through JAK3/STAT3, ERK, and PI3K signaling pathways.[56] Zhang et al reported suppression of NLRP3 inflammasome by dihydroarteannuin via the HIF-1α and JAK3/STAT3 signaling pathway contributed to attenuation of collagen-induced arthritis in mice.[57] The main function of CIS was negative feedback regulation of STAT3. When tacrolimus-induced hepatotoxicity, the expression of CIS was down-regulated, which led to negative feedback failure of STAT3 and failed to inhibit over-activation of JAK3/STAT3 signaling pathway.[58] Wan et al reported the effects of benzene and the metabolites phenol and catechol on c-Myb and PIM1 signaling in HD3 cells, indicating increased expression of PIM1 was associated with hepatotoxicity.[59]

These results suggested that CXCL2-CXCR2 was up-regulated in tacrolimus-induced hepatotoxicity, and the JAK3/STAT3 signaling pathway was activated. In addition, tacrolimus increased the expression of CXCL2-CXCR2 to promote

https://doi.org/10.2147/DDDT.S496195

organ toxicity,[60] however the mechanism for CXCL2-CXCR2 up-regulation by tacrolimus needed further study. Furtherly, we explored the intervention effect of CXCR2 antagonists on tacrolimus-induced hepatotoxicity. In the hepatotoxic group of tacrolimus, ALT, AST, TBIL and MDA were increased, SOD and GSH-Px were decreased, and CXCR2 antagonists could reverse the damage of liver function. In terms of mechanism, after CXCR2 was blocked, the downstream activated JAK3/STAT3 signaling pathway was inhibited, meanwhile, the down-regulated expression of CIS and the up-regulated expression of PIM1 were reversed, and fibrosis related indicators were improved. This furtherly confirmed that CXCR2 blockade was a key point to intervene in tacrolimus-induced hepatotoxicity, and may also be a potential target for drug development.

Conclusion

CXCR2 activated JAK3/STAT3 signaling pathway (p-JAK3/p-STAT3) exacerbating hepatotoxicity associated with tacrolimus, meanwhile, the expression of CIS was down-regulated, the expression of PIM1 was up-regulated. Blocking CXCR2 could reverse the expression of p-JAK3/p-STAT3, CIS, PIM1, and tacrolimus-induced hepatotoxicity.

Data Sharing Statement

All data are available from the corresponding author on reasonable request.

Author Contributions

Xiao Chen and Ke Hu contributed equally to this work and are co-first authors. All authors made a significant contribution to the work reported, whether that is in the conception, study design, execution, acquisition of data, analysis and interpretation, or in all these areas; took part in drafting, revising or critically reviewing the article; gave final approval of the version to be published; have agreed on the journal to which the article has been submitted; and agree to be accountable for all aspects of the work.

Funding

This work was supported by The Natural Science Foundation of Jiangsu Province (No. BK20241046), The Xuzhou Special Fund for Promoting Scientific and Technological Innovation (No. KC23254), The Medical Research Project of Jiangsu Provincial Health Commission (No. Z2023010).

Disclosure

The authors declare that they have no competing interests.

References

1. Bentata Y. Tacrolimus: 20 years of use in adult kidney transplantation. What we should know about its nephrotoxicity. *Artificial Org*. 2020;44(2):140–152. doi:10.1111/aor.13551
2. Andrews LM, de Winter BCM, Cornelissen EAM, et al. A population pharmacokinetic model does not predict the optimal starting dose of tacrolimus in pediatric renal transplant recipients in a prospective study: lessons learned and model improvement. *Clin Pharmacokinet*. 2019;59:591–603.
3. Laub MR, Crow SA, Personett HA, Dierkhising R, Boilson B, Razonable R. Effects of clotrimazole troches on tacrolimus dosing in heart transplant recipients. *Transpl Infect Dis*. 2018;20(6):e12979.
4. Miano TA, Flesch JD, Feng R, et al. Early tacrolimus concentrations after lung transplant are predicted by combined clinical and genetic factors and associated with acute kidney injury. *Clin Pharmacol Ther*. 2020;107(2):462–470. doi:10.1002/cpt.1629
5. Wang D, Chen X, Xu H, Li Z. Population pharmacokinetics and dosing regimen optimization of tacrolimus in Chinese pediatric hematopoietic stem cell transplantation patients. *Xenobiotica*. 2020;50(2):178–185.
6. Wang D, Chen X, Li Z. Treatment of patients with systemic-onset juvenile idiopathic arthritis with tacrolimus. *Exp Ther Med*. 2019;17(3):2305–2309. doi:10.3892/etm.2019.7174
7. Huang L, Wang J, Yang J, et al. Impact of CYP3A4/5 and ABCB1 polymorphisms on tacrolimus exposure and response in pediatric primary nephrotic syndrome. *Pharmacogenomics*. 2019;20(15):1071–1083. doi:10.2217/pgs-2019-0090
8. Kim YH, Shin HY, Kim SM. Long-term safety and efficacy of tacrolimus in myasthenia gravis. *Yonsei Med J*. 2019;60(7):633–639. doi:10.3349/ymj.2019.60.7.633
9. Yanagi T, Ushijima K, Koga H, et al. Tacrolimus for ulcerative colitis in children: a multicenter survey in Japan. *Intest Res*. 2019;17(4):476–485. doi:10.5217/ir.2019.00027

10. Wang DD, Lu JM, Li Q, Li ZP. Population pharmacokinetics of tacrolimus in paediatric systemic lupus erythematosus based on real-world study. *J Clin Pharm Therapeutics*. 2018;43(4):476–483. doi:10.1111/jcpt.12707
11. Hannah J, Casian A, D'Cruz D. Tacrolimus use in lupus nephritis: a systematic review and meta-analysis. *Autoimmunity Rev*. 2016;15(1):93–101. doi:10.1016/j.autrev.2015.09.006
12. Hanouneh M, Ritchie MM, Ascha M. A review of the utility of tacrolimus in the management of adults with autoimmune hepatitis. *Scand J Gastroenterol*. 2019;54(1):76–80. doi:10.1080/00365521.2018.1551498
13. Hoorn EJ, Walsh SB, McCormick JA, et al. The calcineurin inhibitor tacrolimus activates the renal sodium chloride cotransporter to cause hypertension. *Nat Med*. 2011;17(10):1304–1309. doi:10.1038/nm.2497
14. Chen X, Hu K, Shi HZ, et al. Syk/BLNK/NF-kappaB signaling promotes pancreatic injury induced by tacrolimus and potential protective effect from rapamycin. *Biomed Pharmacother*. 2024;171:116125. doi:10.1016/j.biopha.2024.116125
15. Wang D, Chen X, Fu M, Xu H, Li Z. Tacrolimus increases the expression level of the chemokine receptor CXCR2 to promote renal fibrosis progression. *Int J Mol Med*. 2019;44(6):2181–2188. doi:10.3892/ijmm.2019.4368
16. Vecchia Genvigir FD, Campos-Salazar AB, Felipe CR, et al. CYP3A5*3 and CYP2C8*3 variants influence exposure and clinical outcomes of tacrolimus-based therapy. *Pharmacogenomics*. 2020;21(1):7–21. doi:10.2217/pgs-2019-0120
17. Campagne O, Mager DE, Tornatore KM. Population pharmacokinetics of tacrolimus in transplant recipients: what did we learn about sources of interindividual variabilities? *J Clin Pharmacol*. 2019;59(3):309–325. doi:10.1002/jcph.1325
18. Hu K, Fu M, Huang X, He S, Jiao Z, Wang D. Editorial: model-informed drug development and precision dosing in clinical pharmacology practice. *Front Pharmacol*. 2023;14:1224980. doi:10.3389/fphar.2023.1224980
19. Wang DD, Mei YQ, Yang L, et al. Optimization of initial dose regimen of tacrolimus in paediatric lung transplant recipients based on monte carlo simulation. *J Clin Pharm therapeutics*. 2022;47(10):1659–1666. doi:10.1111/jcpt.13717
20. Chen X, Wang DD, Xu H, Li ZP. Population pharmacokinetics and pharmacogenomics of tacrolimus in Chinese children receiving a liver transplant: initial dose recommendation. *Transl Pediatr*. 2020;9(5):576–586. doi:10.21037/tp-20-84
21. Chen X, Wang DD, Xu H, Li ZP. Initial dosage optimization of tacrolimus in Chinese pediatric patients undergoing kidney transplantation based on population pharmacokinetics and pharmacogenetics. *Expert Rev Clin Pharmacol*. 2020;13(5):553–561. doi:10.1080/17512433.2020.1767592
22. Chen X, Wang D, Zheng F, et al. Effects of posaconazole on tacrolimus population pharmacokinetics and initial dose in children with crohn's disease undergoing hematopoietic stem cell transplantation. *Front Pharmacol*. 2022;13:758524. doi:10.3389/fphar.2022.758524
23. Chen X, Wang D, Lan J. Effects of voriconazole on population pharmacokinetics and optimization of the initial dose of tacrolimus in children with chronic granulomatous disease undergoing hematopoietic stem cell transplantation. *Ann Transl Med*. 2021;9(18):1477. doi:10.21037/atm-21-4124
24. Chen X, Wang D, Zheng F, Zhai X, Xu H, Li Z. Population pharmacokinetics and initial dose optimization of tacrolimus in children with severe combined immunodeficiency undergoing hematopoietic stem cell transplantation. *Front Pharmacol*. 2022;13:869939. doi:10.3389/fphar.2022.869939
25. Ferjani H, El Arem A, Bouraoui A, et al. Protective effect of mycophenolate mofetil against nephrotoxicity and hepatotoxicity induced by tacrolimus in Wistar rats. *J Physiol Biochem*. 2016;72(2):133–144. doi:10.1007/s13105-015-0451-7
26. Ko MS, Choi YH, Jung SH, et al. Tacrolimus therapy causes hepatotoxicity in patients with a history of liver disease. *Int J Clin Pharmacol Ther*. 2015;53(5):363–371. doi:10.5414/CP202226
27. Koc S, Aktas A, Sahin B, Ozer H, Zararsiz GE. Protective effect of ursodeoxycholic acid and resveratrol against tacrolimus induced hepatotoxicity. *Biotech Histochem*. 2023;98(7):471–478. doi:10.1080/10520295.2023.2228697
28. Mesar I, Kes P, Hudolin T, Basic-Jukic N. Rescue therapy with sirolimus in a renal transplant recipient with tacrolimus-induced hepatotoxicity. *Ren Fail*. 2013;35(10):1434–1435. doi:10.3109/0886022X.2013.828356
29. Sacher VY, Bejarano PA, Pham SM. Tacrolimus induced hepatotoxicity in a patient with bilateral lung transplant. *Transpl Int*. 2012;25(10):e111–2. doi:10.1111/j.1432-2277.2012.01546.x
30. Terzi F, Ciftci MK. Protective effect of silymarin on tacrolimus-induced kidney and liver toxicity. *BMC Complement Med Ther*. 2022;22(1):331. doi:10.1186/s12906-022-03803-x
31. Denton MD, Magee CC, Sayegh MH. Immunosuppressive strategies in transplantation. *Lancet*. 1999;353(9158):1083–1091.
32. Greenbaum LA, Benndorf R, Smoyer WE. Childhood nephrotic syndrome--current and future therapies. *Nat Rev Nephrology*. 2012;8(8):445–458. doi:10.1038/nrneph.2012.115
33. Moller A, Iwasaki K, Kawamura A, et al. The disposition of 14C-labeled tacrolimus after intravenous and oral administration in healthy human subjects. *Drug Metab Dispos*. 1999;27(6):633–636.
34. Wallemacq PE, Furlan V, Moller A, et al. Pharmacokinetics of tacrolimus (FK506) in paediatric liver transplant recipients. *Eur J Drug Metab Pharmacokinet*. 1998;23(3):367–370. doi:10.1007/BF03192295
35. Kay JE, Sampare-Kwateng E, Geraghty F, Morgan GY. Uptake of FK 506 by lymphocytes and erythrocytes. *Transplant Proc*. 1991;23(6):2760–2762.
36. Plekoszewski W, Jusko WJ. Plasma protein binding of tacrolimus in humans. *J Pharm Pharm Sci*. 1993;82(3):340–341. doi:10.1002/jps.2600820325
37. Chen B, Shi HQ, Liu XX, et al. Population pharmacokinetics and bayesian estimation of tacrolimus exposure in Chinese liver transplant patients. *J Clin Pharm Therapeutics*. 2017;42(6):679–688. doi:10.1111/jcpt.12599
38. Moes DJ, van der Bent SA, Swen JJ, et al. Population pharmacokinetics and pharmacogenetics of once daily tacrolimus formulation in stable liver transplant recipients. *Eur J Clin Pharmacol*. 2016;72(2):163–174. doi:10.1007/s00228-015-1963-3
39. Woillard JB, Debord J, Monchaud C, Saint-Marcoux F, Marquet P. Population pharmacokinetics and bayesian estimators for refined dose adjustment of a new tacrolimus formulation in kidney and liver transplant patients. *Clin Pharmacokinet*. 2017;56(12):1491–1498. doi:10.1007/s40262-017-0533-5
40. Zhang HJ, Li DY, Zhu HJ, Fang Y, Liu TS. Tacrolimus population pharmacokinetics according to CYP3A5 genotype and clinical factors in Chinese adult kidney transplant recipients. *J Clin Pharm Therapeutics*. 2017;42(4):425–432. doi:10.1111/jcpt.12523
41. Cheng Y, Ma XL, Wei YQ, Wei XW. Potential roles and targeted therapy of the CXCLs/CXCR2 axis in cancer and inflammatory diseases. *Biochimica et biophysica acta Rev Cancer*. 2019;1871(2):289–312. doi:10.1016/j.bbcan.2019.01.005

42. Romero-Moreno R, Curtis KJ, Coughlin TR, et al. The CXCL5/CXCR2 axis is sufficient to promote breast cancer colonization during bone metastasis. *Nat Commun*. 2019;10(1):4404. doi:10.1038/s41467-019-12108-6
43. Jin L, Tao H, Karachi A, et al. CXCR1- or CXCR2-modified CAR T cells co-opt IL-8 for maximal antitumor efficacy in solid tumors. *Nat Commun*. 2019;10(1):4016. doi:10.1038/s41467-019-11869-4
44. Dart A. Metastasis: CXCR2-targeted therapy for pancreatic cancer. *Nat rev Cancer*. 2016;16(7):411.
45. Shang FM, Li J. A small-molecule antagonist of CXCR1 and CXCR2 inhibits cell proliferation, migration and invasion in melanoma via PI3K/AKT pathway. *Med clinica*. 2019;152(11):425–430. doi:10.1016/j.medcli.2018.08.006
46. Wang Y, Tu L, Du C, et al. CXCR2 is a novel cancer stem-like cell marker for triple-negative breast cancer. *Onco Targets Ther*. 2018;11:5559–5567. doi:10.2147/OTT.S174329
47. Cong L, Qiu ZY, Zhao Y, et al. Loss of beta-arrestin-2 and activation of CXCR2 correlate with lymph node metastasis in non-small cell lung cancer. *J Cancer*. 2017;8(14):2785–2792. doi:10.7150/jca.19631
48. Stofas A, Levidou G, Piperi C. The role of CXC-chemokine receptor CXCR2 and suppressor of cytokine signaling-3 (SOCS-3) in renal cell carcinoma. *BMC Cancer*. 2014;14:149. doi:10.1186/1471-2407-14-149
49. Gao Y, Guan Z, Chen J, et al. CXCL5/CXCR2 axis promotes bladder cancer cell migration and invasion by activating PI3K/AKT-induced upregulation of MMP2/MMP9. *Int J Oncol*. 2015;47(2):690–700. doi:10.3892/ijo.2015.3041
50. Di Mitri D, Mirenda M, Vasilevska J, et al. Re-education of tumor-associated macrophages by cxcr2 blockade drives senescence and tumor inhibition in advanced prostate cancer. *Cell Rep*. 2019;28(8):2156–2168e5. doi:10.1016/j.celrep.2019.07.068
51. Ogawa R, Yamamoto T, Hirai H, et al. Loss of SMAD4 promotes colorectal cancer progression by recruiting tumor-associated neutrophils via the CXCL1/8-CXCR2 axis. *Clin Cancer Res*. 2019;25(9):2887–2899. doi:10.1158/1078-0432.CCR-18-3684
52. Dornelles FN, Andrade EL, Campos MM, Calixto JB. Role of CXCR2 and TRPV1 in functional, inflammatory and behavioural changes in the rat model of cyclophosphamide-induced haemorrhagic cystitis. *Br J Pharmacol*. 2014;171(2):452–467. doi:10.1111/bph.12467
53. Ranganathan P, Jayakumar C, Manicassamy S, Ramesh G. CXCR2 knockout mice are protected against DSS-colitis-induced acute kidney injury and inflammation. *Am J Physiol Renal Physiol*. 2013;305(10):F1422–7. doi:10.1152/ajprenal.00319.2013
54. Xiao T, Cheng X, Zhi Y, et al. Ameliorative effect of alangium chinense (Lour.) harms on rheumatoid arthritis by reducing autophagy with targeting regulate JAK3-STAT3 and COX-2 pathways. *J Ethnopharmacol*. 2024;319(Pt 1):117133. doi:10.1016/j.jep.2023.117133
55. Zhang J, Liu T, Duan Y, et al. Single-cell analysis highlights a population of Th17-polarized CD4(+) naive T cells showing IL6/JAK3/STAT3 activation in pediatric severe aplastic anemia. *J Autoimmun*. 2023;136:103026. doi:10.1016/j.jaut.2023.103026
56. Fathi E, Mesbah-Namin SA, Vietor I, Farahzadi R. Mesenchymal stem cells cause induction of granulocyte differentiation of rat bone marrow C-kit (+) hematopoietic stem cells through JAK3/STAT3, ERK, and PI3K signaling pathways. *Iran J Basic Med Sci*. 2022;25(10):1222–1227. doi:10.22038/IJBMS.2022.66737.14633
57. Zhang M, Wu D, Xu J, et al. Suppression of NLRP3 inflammasome by dihydroarteannuin via the HIF-1alpha and JAK3/STAT3 signaling pathway contributes to attenuation of collagen-induced arthritis in mice. *Front Pharmacol*. 2022;13:884881. doi:10.3389/fphar.2022.884881
58. Yoshimura A. The CIS family: negative regulators of JAK-STAT signaling. *Cytokine Growth Factor Rev*. 1998;9(3–4):197–204. doi:10.1016/S1359-6101(98)00019-7
59. Wan J, Winn LM. The effects of benzene and the metabolites phenol and catechol on c-Myb and Pim-1 signaling in HD3 cells. *Toxicol Appl Pharmacol*. 2004;201(2):194–201. doi:10.1016/j.taap.2004.05.010
60. Chen X, Hu K, Zhang Y, He SM, Wang DD. Targeting CXCR2 ameliorated tacrolimus-induced nephrotoxicity by alleviating overactivation of PI3K/AKT/mTOR pathway and calcium overload. *Biomed Pharmacother*. 2024;180:117526. doi:10.1016/j.biopha.2024.117526